Received: 26 October 2018 | Revised: 25 March 2019 | Accepted: 31 March 2019

DOI: 10.1002/ardp.201800314

FULL PAPER

DPhG ARCH PHARM
Archiv der Pharmazie

Utility of anthranilic acid and diethylacetylenedicarboxylate for the synthesis of nitrogenous organo/organometallic compounds as urease inhibitors

Heba S. A. El-Zahabi[1] | Hanan G. Abdulwahab[1] | Mastoura M. Edrees[2,3] | Amany M. Hegab[4]

[1]Department of Pharmaceutical Chemistry, Faculty of Pharmacy (Girls), Al-Azhar University, Cairo, Egypt

[2]Department of Organic Chemistry, National Organization for Drug Control and Research, Giza, Egypt

[3]Department of Chemistry, Faculty of Science, King Khalid University, Abha, Saudi Arabia

[4]Developmental Pharmacology Department, National Organization for Drug Control and Research, Giza, Egypt

Correspondence
Hanan Gaber Abdulwahab, Department of Pharmaceutical Chemistry, Faculty of Pharmacy (Girls), Al-Azhar University, Cairo 11754, Egypt.
Email: hanangaber@azhar.edu.eg

Abstract

Fumarate diester **3** was synthesized upon reacting anthranilic acid with diethylacetylenedicarboxylate. Compound **3** was reacted with different nucleophiles in mild reaction conditions. Selected reaction routes that afforded products **6**, **9**, **10**, **11**, and **12** were explained. The estimated mechanism for the reaction of **3** with ethylenediamine to afford **9** was proved by X-ray single-crystal and retro-synthetic reaction. Acetyl anthranilic acid was utilized with zinc and copper to afford the organometallic compounds **14a** and **14b**, respectively. Three single crystals were afforded for **3**, **9** and the organocopper complex **14b**. Target compounds were screened for their inhibitory potential against urease enzyme. Most compounds were more potent than thiourea as standard inhibitor, considering that oxopiperazine **9** exhibited double the activity: IC_{50} = 8.16 ± 0.65 μM (thiourea IC_{50} = 20.04 ± 0.33 μM). Docking studies were in agreement with the in vitro enzyme assay.

KEYWORDS

anthranilic acid, diethylacetylenedicarboxylate, docking study, organometallic, single crystal, urease inhibitor

1 | INTRODUCTION

Urease is a nickel-based metalloenzyme that catalyzes the hydrolysis of urea into carbon dioxide and ammonia. Ureases are widely found in various organisms including bacteria, fungi, and plants. Although having different origin, all known ureases share at least 50% identity, possess common amino acid sequences in the active site and thus show same catalytic mechanism.[1] Production of ammonia from urease is responsible for harmful complications in health fields. The pathogenesis of many clinical conditions, such as peptic ulcer caused by *Helicobacter pylori*, hepatic coma, pyelonephritis, and infection-induced urinary stones are related to the ureolytic activity of microbial enzymes.[2,3] Thus, searching for urease inhibitor drugs is an important target in controlling infections caused by urease-producing bacteria. These inhibitors play an important role in controlling ureolytic microorganisms, and also help exploring and understanding novel aspects of the mechanism of action of ureases.[4,5]

Anthranilic acid has an old history as a chemical precursor for many organic bioactive compounds; for example, diuretics, antioxidants, antiproliferative and antiallergic agents.[6–9] Furthermore, Rauf et al.[10] reported the urease inhibitory activity of diverse substituted aniline based thiobarbiturates, among which the anthranilic acid derivative **I** displayed potent urease inhibitory activity with IC_{50} = 12.96 ± 0.13 μM compared to thiourea as reference standard (IC_{50} = 21 ± 0.011 μM) (Figure 1). Also, the importance of unsaturated carbonyl compounds as urease inhibitors was illustrated in many literatures.[11–13] Recently, Macegoniuk et al.[14] described the potent urease inhibitory activity of several unsaturated carbonyl compounds, with acetylenedicarboxylic acid **II**, and dimethylacetylenedicarboxylate **III** (Figure 1) being the most potent. Additionally, benzimidazole-based antiulcer drug, rabeprazole,[15,16] various

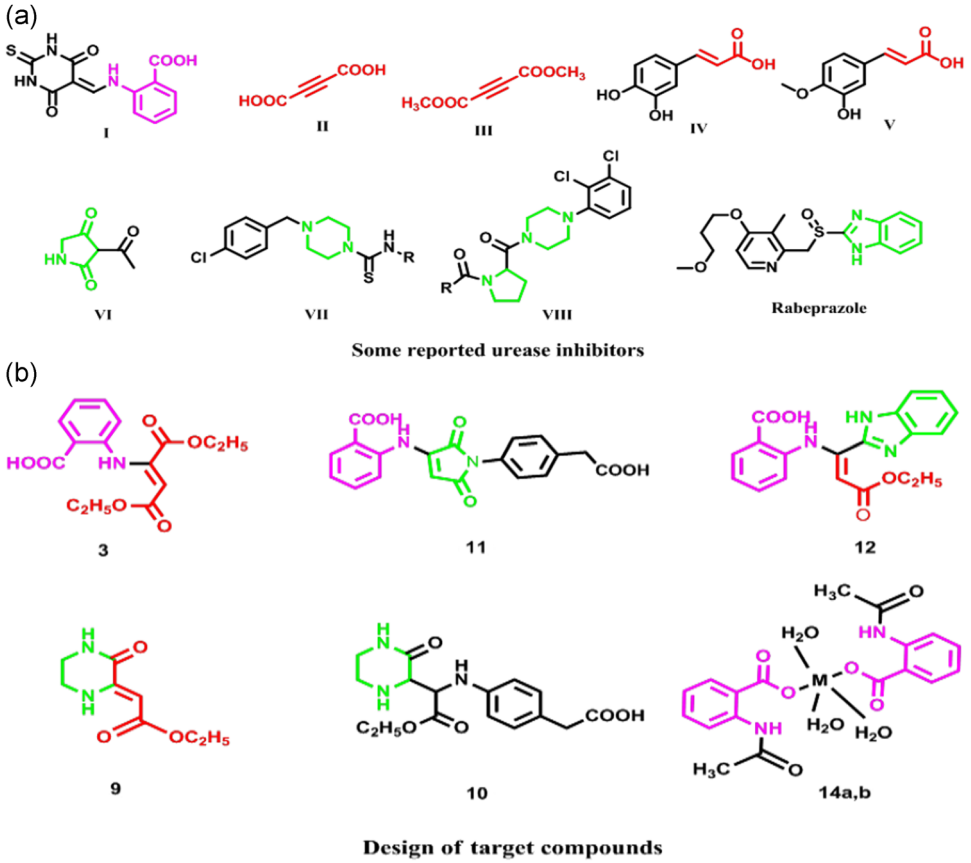

FIGURE 1 Structural similarities between some reported urease inhibitors (a) and target compounds (b)

carboxylic acids,[12,13,17] piperazine derivatives,[18,19] dioxopyrroles,[13] and metal complexes[12,13,20,21] displayed potent urease inhibitory activity (Figure 1).

From a chemical point of view, the conjugation between the diester moiety and the acetylene system of dimethylacetylenedicarboxylate (DMAD) explored various chemical reactivities. Several research groups investigated the reaction of DMAD with numerous nucleophiles, illustrating different pathways, either attacking the acetylene moiety or the ester function. These previous reactions covered broad estimated mechanisms, afforded various heterorganic compounds, and were noticeably affected by solvent, temperature, and the nature of the basic reactants.[22–27]

Motivated by these findings, diethylacetylenedicarboxylate (DEAD) was reacted with anthranilic acid, to afford aryl/heteroaryl and alicyclic derivatives of expected urease inhibitory activity. Additionally, metal complexation reactions of anthranilic acid with zinc and copper were carried out to explore the antiurease activity of the afforded organometallic complexes.

2 | RESULTS AND DISCUSSION

2.1 | Chemistry

Synthesis of dimethoxy-dioxobutenylamino benzoic acid was reported by Khetan et al.,[28] via stirring anthranilic acid with dimethylacetylenedicarboxylate in methanol at room temperature for 1 hr. Herein, the new diethoxy analog **3** was afforded by stirring anthranilic acid **1** with DEAD **2** adopting the reported procedure,[28] using ethanol as a solvent. Anthranilic acid **1** initiated the reaction by α

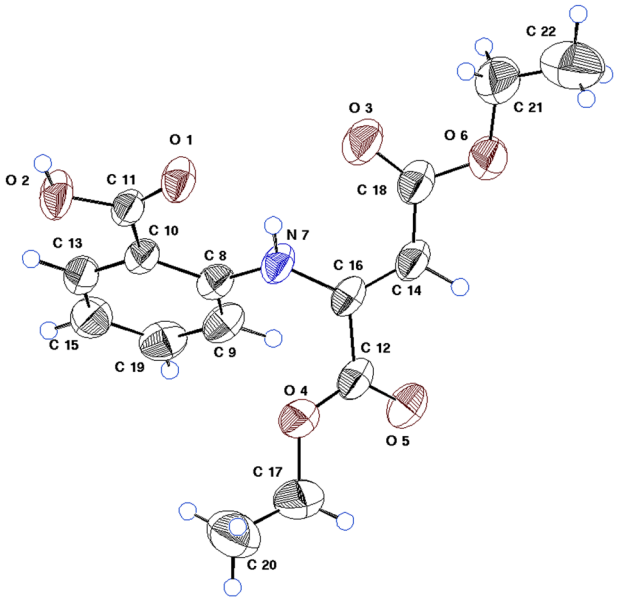

FIGURE 2 Molecular structure of compound **3** with anisotropic displacement ellipsoids drawn at the 50% probability level

and β nucleophilic addition on the triple bond rather than the aminolysis of the ester function of compound **2**. The infrared radiation (IR), mass spectrometry (MS) and ^{1}H nuclear magnetic resonance (NMR) spectra proved the assigned structure of compound **3**. IR spectrum of **3** showed the presence of two carbonyl absorptions at 1728, 1680 (ester C=O), and 1670 (acid C=O) cm^{-1}. ^{1}H NMR spectra revealed the appearance of four signals δ 1.04 (t), 1.10 (t), 4.08–4.17 (m) due to the diethyl ester protons. Also, a singlet appeared at δ 5.43 ppm for the vinyl resonance. The mass spectrum showed the presence of *m/z* at 307 due to the molecular ion peak (M^+). Compound **3** was also proved by single crystal X-ray analysis as depicted in Figure 2, Table 1. To illustrate the reactivity of the diethyl fumarate analog **3**, nucleophilic reactions with different amines were carried out. The point of the investigation was to detect the position of attack, either α,β addition on the double bond or direct aminolysis of the ester function. The reaction proceeded in polar protic solvent for example, ethanol under reflux with TLC follow-up. As a starting point, compound **3** was treated with hydrazine hydrate in ethanol under reflux in 1:5 mole equivalence, respectively. Interestingly, the structure of the product **4** was ruled out according to the spectral data that explored complete disappearance of the signals corresponding for the aromatic protons. Since a variety of products, for example,

TABLE 1 Main bond geometries (lengths and angles) for compounds **3**, **9**, **14b**

	3		**9**		**14b**	
Bond length (Å)						
	O1—C11	1.235 (4)	O1—C8	1.351 (3)	Cu1—O2	1.905 (2)
	O2—C11	1.310 (4)	O1—C12	1.455 (4)	Cu1—O4	1.962 (3)
	O3—C18	1.211 (4)	O2—C6	1.240 (3)	Cu1—O5	1.993 (2)
	O4—C12	1.328 (5)	N3—C6	1.322 (4)	Cu1—O6	1.928 (2)
	O4—C17	1.459 (6)	N3—C11	1.454 (4)	Cu1—O9	2.275 (3)
	O5—C12	1.204 (4)	O4—C8	1.225 (4)	O2—C17	1.308 (4)
	O6—C18	1.343 (5)	C5—C6	1.502 (4)	O3—C17	1.237 (4)
	N7—C8	1.402 (5)	C5—N7	1.346 (4)	O6—C12	1.287 (4)
	N7—C16	1.375 (4)	C5—C10	1.353 (4)	N11—C16	1.429 (5)
	C10—C11	1.465 (5)	N7—C9	1.446 (4)	C13—C17	1.482 (5)
	C12—C16	1.503 (6)	C8—C10	1.433 (4)	N15—C21	1.390 (5)
	C14—C16	1.343 (5)	C9—C11	1.469 (5)	N15—C22	1.366 (5)
	C14—C18	1.449 (6)	C12—C13	1.474 (5)	O18—C19	1.204 (5)
	O2—H2	0.960 (3)	C9—H9A	0.960 (3)	C19—C28	1.520 (6)
	N7—H7	0.960 (3)	C11—H11A	0.960 (4)	O20—C22	1.236 (5)
Bond angle (°)						
	C12—O4—C17	115.8 (3)	C8—O1—C12	116.2 (3)	O2—Cu1—O4	89.15 (11)
	C8—N7—C16	125.8 (3)	C6—N3—C11	123.3 (3)	O2—Cu1—O5	92.77 (11)
	N7—C8—C9	121.2 (3)	C6—C5—N7	118.0 (3)	O2—Cu1—O6	173.04 (11)
	C8—C10—C11	122.4 (3)	N7—C5—C10	124.6 (3)	O2—Cu1—O9	87.36 (10)
	C8—C10—C13	118.9 (3)	O2—C6—N3	122.5 (3)	O4—Cu1—O5	157.74 (12)
	O1—C11—O2	121.4 (3)	N3—C6—C5	117.0 (3)	O4—Cu1—O6	89.27 (11)
	O4—C12—O5	124.6 (4)	C5—N7—C9	121.8 (3)	O4—Cu1—O9	110.51 (11)
	O4—C12—C16	111.5 (3)	O1—C8—O4	122.5 (3)	O5—Cu1—O6	91.26 (11)
	C16—C14—C18	123.9 (3)	N7—C9—C11	110.6 (3)	O5—Cu1—O9	91.74 (11)
	N7—C16—C14	123.7 (4)	C5—C10—C8	123.6 (3)	O6—Cu1—O9	86.84 (11)
	C12—C16—C14	116.2 (3)	N3—C11—C9	111.2 (3)	Cu1—O2—C17	128.3 (2)
	O4—C17—C20	109.2 (4)	O1—C12—C13	107.4 (3)	Cu1—O6—C12	124.8 (2)
	H17A—C17—H17B	109.5 (5)	N7—C9—H9B	109.6 (3)	C12—C10—C21	124.6 (3)
	O3—C18—O6	122.6 (4)	C11—C9—H9A	110.4 (3)	C16—N11—C19	129.3 (3)
	O6—C18—C14	111.5 (3)	H9A—C9—H9B	109.5 (3)	C21—N15—C22	131.3 (4)
	C8—N7—H7	119.6 (3)	N3—C11—H11B	107.9 (3)	N11—C19—O18	125.5 (4)
	H20A—C20—H20B	109.5 (6)	C9—C11—H11A	110.5 (4)	N15—C22—O20	122.1 (4)
	H21A—C21—H21B	109.5 (5)	H11A-C11-H11B	109.5 (4)	H26A-C26-H26B	109.5 (5)

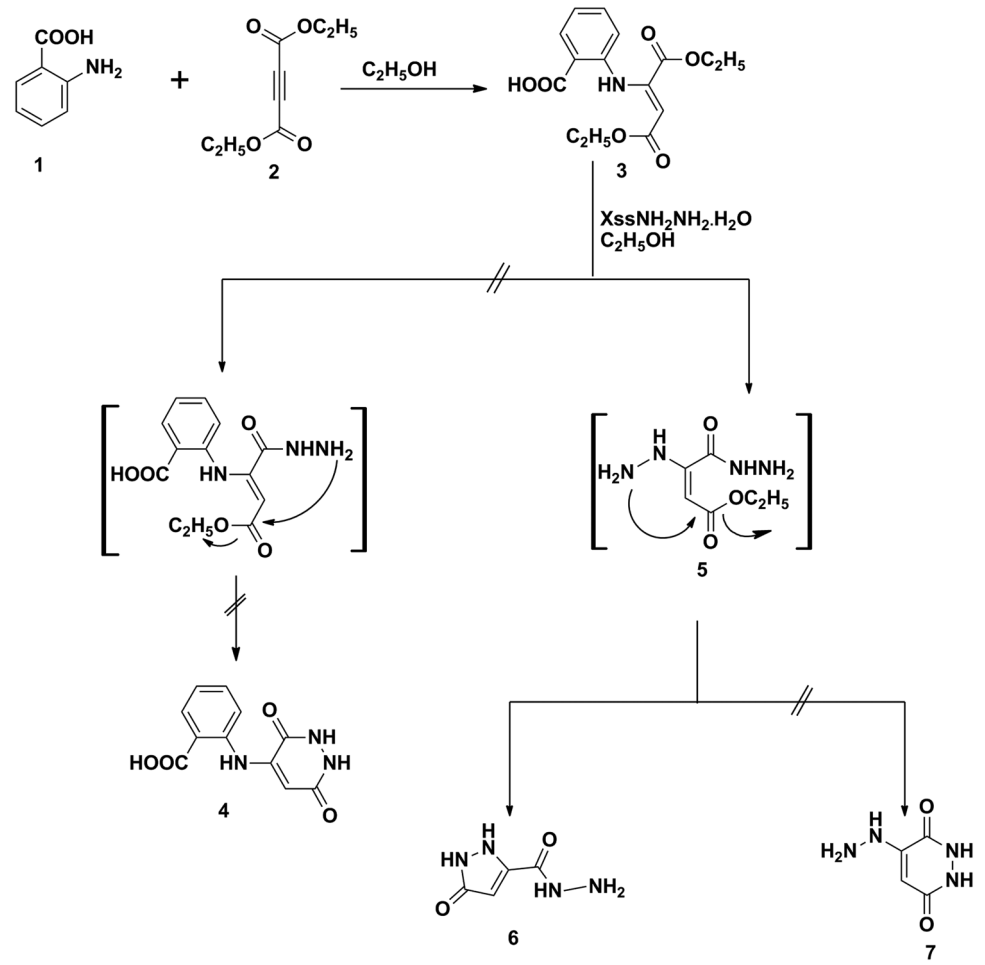

SCHEME 1 Synthesis of compounds **3** and **6**

4, **6**, were suggested, yet the reaction was estimated to proceed via displacement of the aminobenzoic acid moiety with hydrazinolysis of one ethoxide moiety, consuming two moles of hydrazine hydrate. Sequentially, nucleophilic attack of the hydrazinyl moiety neighboring to carbonyl group in intermediate **5** afforded the pyrazole carbohydrazide derivative **6**. Suggested product **6** was concomitant to the pattern of Heindel et al.[29] Pyrazole carbohydrazide **6** was preferentially suggested rather than pyridazindione compound **7.** The cyclization route according to Heindel et al.[29] was found to afford pyrazolin-5-one analog with ^{1}H NMR signal at δ 5.97 ppm for the vinyl resonance. Additionally, Wu et al.[30] reported the existence of the vinyl resonance of pyridazin-3-one ring at lower field, for example, 7.15 ppm. Herein, ^{1}H NMR analysis was in complete agreement with structure **6**, illustrating the signal of the vinyl proton at the upper field of δ 5.96 ppm. Simultaneously, ^{13}C NMR spectrum supported the structure of **6** rather than pyridazindione **7**. Actually, the observed ^{13}C NMR spectrum revealed two close signals at δ 161.41 and 161.83 ppm (2CO). Concomitantly, two additional signals appeared at δ 141.47 and 86.70 ppm assigned for C3 and C4 of pyrazoline ring, respectively (Scheme 1).

Simultaneously, diethoxy analog **3** was treated with equimolar equivalence of ethylenediamine, applying the previously mentioned condition. A similar mechanistic pathway was assumed via displacement of aminobenzoic acid moiety to afford enamine intermediate **8** that constituted a ready synthesis of piperazine analog **9**. IR, MS, and ^{1}H NMR spectra of the isolated product greatly supported the assigned structure **9**. IR spectrum showed the presence of two carbonyl absorptions at 1689 and 1658 cm^{-1}. ^{1}H NMR spectrum revealed the appearance of three signals at δ 1.15 (t), 3.25–3.29 (m) and 4.04 (q) ppm due to the ethyl group of ester and two methylene protons of piperazine. Finally, the vinyl resonance appeared at 5.16 (s) ppm. The mass spectrum showed the presence of *m/z* at 184 due to the molecular ion peak (M^{+}). The structure of compound **9** was unequivocally determined by single crystal X-ray analysis as depicted in Figure 3, Table 1. Further, applying the retro-synthetic route of compound **9** that reported by Iwanami et al.[31] was an additional confirmative tool for the estimated reaction mechanism between ethylenediamine and precursor **3** (Scheme 2). Focusing on the oxo-α,β-unsaturated ester entity of **9**, two reactive sites were explored, either olefinic bond or ester moiety. Consequently, nucleophilic addition of *p*-aminophenyl acetic acid on olefinic bond of oxopiperazinylidene acetate **9** was carried out, adopting the study done by Medvedeva et al.[32] So, the reaction was carried out in ethanol under reflux to afford the

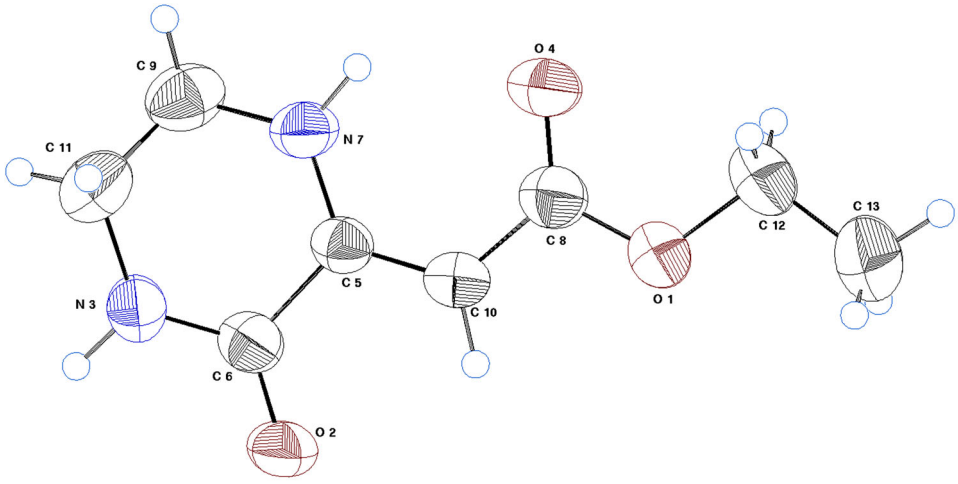

FIGURE 3 Molecular structure of compound **9** with anisotropic displacement ellipsoids drawn at the 50% probability level

enamine isomer (**I**) rather than imine isomer (**II**) (Figure 4). Reported literature[33] confirmed the aminolysis of α,β-unsaturated ester by using excess amine under fusion, herein, the reaction was applied using double mole equivalence of *p*-aminophenyl acetic acid in ethanol under reflux condition (TLC follow-up). Interestingly, nucleophilic addition on olefinic bond was afforded rather than aminolysis of the ester function to yield compound **10**., Its structure was proved by elemental and spectral data (see experimental section). The mass spectrum showed the presence of *m/z* at 335 due to the molecular ion peak (M^+).

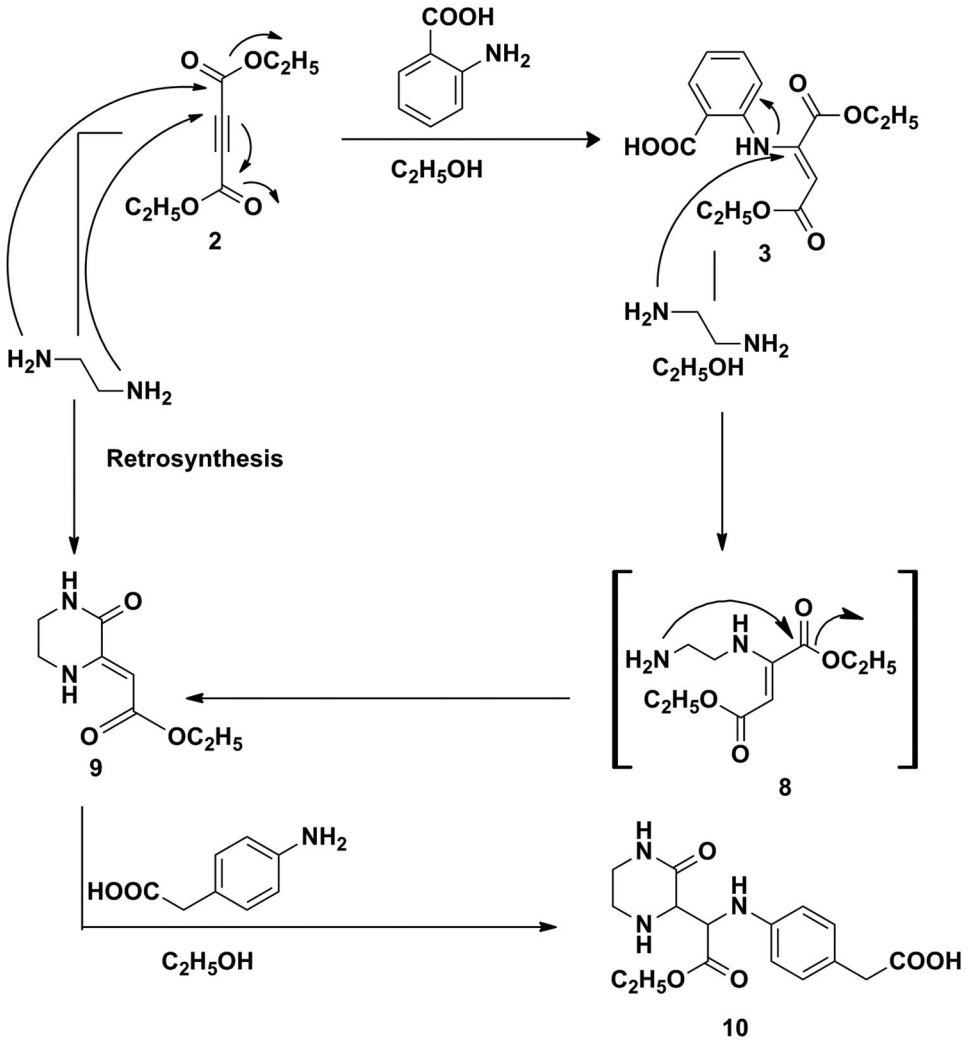

SCHEME 2 Synthesis of compounds **9** and **10**

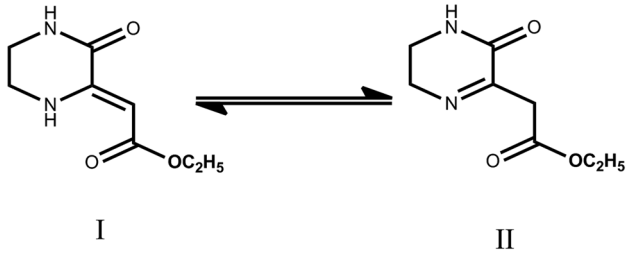

FIGURE 4 Estimated isomeric forms **I** and **II** of compound **9**

In the next step, the diethoxy analog **3** was treated with aromatic amines (Scheme 3). In contrast to ethylenediamine in Scheme 1, the applied aromatic amines could not replace the aminobenzoic acid moiety. So, analog **3** was reacted with equimolar equivalence of either *p*-aminophenyl acetic acid or *o*-phenylenediamine in ethanol under reflux to afford the corresponding heterocyclic analogs **11** and **12**, respectively. Noticeably, the reported reaction of diethyl fumarate with amines proceeded mainly via Micheal addition and aminolysis.[34] Compound **11** was afforded via aminolysis of the two ethoxide groups, consuming one mole of *p*-aminophenyl acetic acid. The IR, MS and ^{1}H NMR spectra of the isolated product greatly supported the assigned structure **11**. ^{1}H NMR spectrum revealed the disappearance of the protons of the ester functions. Concomitantly, the methylenic protons of acetic acid moiety appeared at 3.37 ppm. The vinyl resonance displayed a singlet signal at 5.78 ppm. A multiplet for the aromatic protons appeared at 7.18–7.40 ppm. ^{13}C NMR spectrum revealed a signal at 40.59 ppm for methylenic carbon of acetic acid moiety. Also, four signals appeared at 167.01, 172.00, 173.14, and 173.82 for (CO) (see Section 4). The mass spectrum showed the presence of *m/z* at 366 due to the molecular ion peak (M^+). The reaction of *o*-phenylenediamine with precursor **3** provided aminolysis of one ethoxide group followed by intramolecular cyclocondensation to afford the benzimidazole derivative **12**. The structure of **12** was established on the basis of its elemental analysis and spectral data (see Section 4).

Moreover, the utility of anthranilic acid scaffold was extended to apply complexation of the acetyl anthranilic acid with copper and zinc metals adopting the reported procedures.[35,36] The complexation proceeded via mixing ethanolic solution of the acetyl anthranilic acid **13** with aqueous suspension of $Zn(OH)_2$ or solution of $CuSO_4$ to afford the corresponding complex **14a** and **14b**, respectively (Scheme 4). The structure of bis(2-acetylaminobenzoato)Cu(II) **14b** was confirmed by single crystal X-ray analysis as depicted in Figure 5, Table 1.

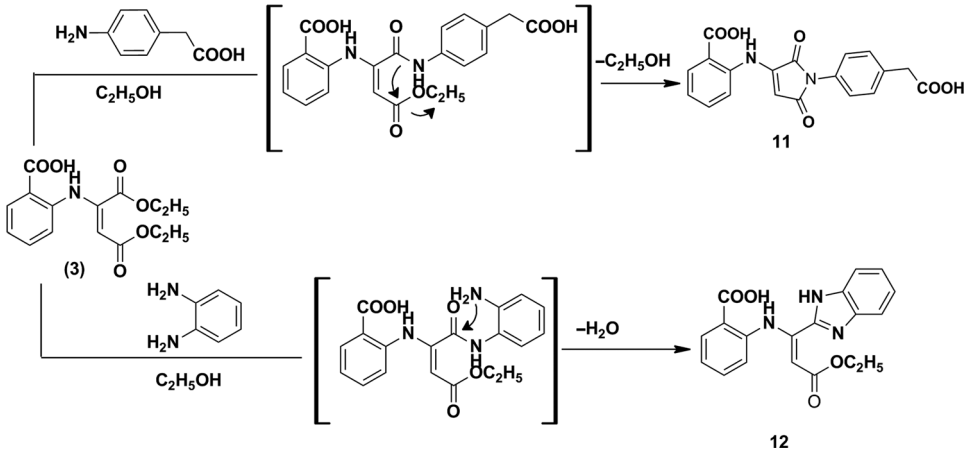

SCHEME 3 Synthesis of compounds **11** and **12**

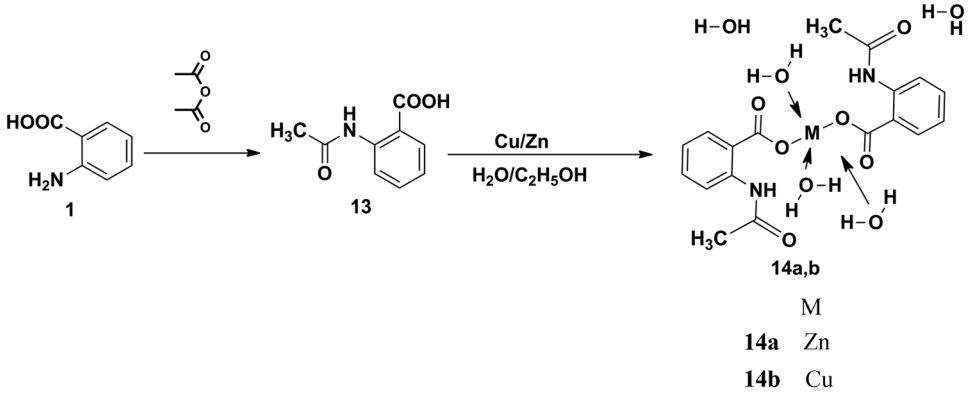

SCHEME 4 Synthesis of compounds **14a,b**

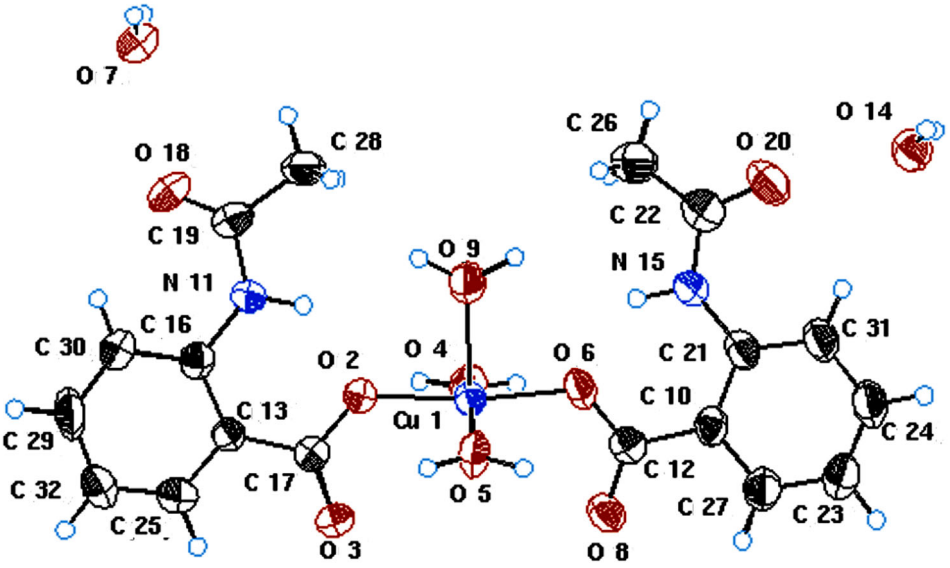

FIGURE 5 Molecular structure of compound **14b** with anisotropic displacement ellipsoids drawn at the 50% probability level

2.2 | In vitro urease inhibition assay

Among numerous ureases, jack bean (*Canavalia ensiformis*) urease, the first enzyme crystallized[37] and best-characterized,[38–40] has been widely utilized in urease inhibition studies.[41,42] Accordingly, the newly synthesized compounds, namely, **3**, **9**, **10**, **11**, **12**, and **14a**,**b** were screened for their inhibitory potential against jack bean urease using thiourea as a standard inhibitor. Screening results revealed that compounds **3**, **9–11**, and **14a** demonstrated diverse antiurease activity having IC_{50} values in a range of 8.16 ± 0.65 to 46.91 ± 0.08 μM compared to thiourea of IC_{50} value 20.04 ± 0.33 μM. Compounds **3**, **9–11** were found to be the most active and superior to the standard inhibitor (Table 2). Among the tested compounds, oxopiperazine **9** was the most potent, compared to the reference standard. It exhibited double the activity of thiourea with IC_{50} 8.16 ± 0.65 and 20.04 ± 0.33 μM, respectively. Compounds **3**, **10**, and **11** were almost equipotent with IC_{50} 14.13 ± 4.16, 14.09 ± 0.49, and 13.68 ± 0.67 μM, respectively. Zinc complex **14a** exhibited almost half the activity of thiourea with IC_{50} 46.91 ± 0.08 μM. On the other hand, copper complex **14b** and benzimidazole derivative **12** showed no inhibitory activity against urease enzyme.

TABLE 2 In vitro urease inhibitory activity of tested compounds compared to thiourea

Compound no.	IC_{50} ± SEM (μM)
3	14.13 ± 4.16
9	8.16 ± 0.65
10	14.09 ± 0.49
11	13.68 ± 0.67
12	NA
14a	46.91 ± 0.08
14b	NA
Thiourea[a]	20.04 ± 0.33

Note. NA: no activity; SEM: standard error of the mean.
Result represented as mean of triplicate ± SEM.
[a]Thiourea standard inhibitor for antiurease activity.

2.3 | Structure–activity relationships

Herein, we have synthesized some new compounds in which different antiurease scaffolds were incorporated. Also, the molecular hybridization approach was considered. Thus, anthranilic acid scaffold was hybridized with fumarate diester in compound **3**. It was also linked to pyrrole and benzimidazole scaffolds in **11** and **12**, respectively. Piperazine scaffold was hybridized with fumarate diester in compound **9.** Based on the design of our target compounds (Figure 1), the test compounds **3**, **9–11**, **14a**,**b** could be structurally classified as anthranilic acid analogs **3**, **11**, **12**, oxopiperazines **9** and **10**, and metalloanthranilic acid complexes **14a**,**b.** Structurally, replacing one sided amino group of thiourea by oxopiperazinylidene moiety afforded compound **9**, which greatly exceeded thiourea as urease inhibitor. Focusing on anthranilic acid analogs **3**, **11**, **12**, the fumarate ester **3**, and the dioxopyrrole **11** almost showed the same activity. The rigid diethoxyfumarate moiety in **3** was replaced by *N*-phenyl dioxopyrrole ring in **11**, considering the hydrophilic carboxymethyl moiety in the *para*-position. Noticeably, this structural modification did not affect urease inhibitory activity. However, replacing the carboxyethyl moiety in **3** by benzimidazole ring in **12** afforded complete loss of antiurease activity. Khan et al.[43] reported weak antiurease activity of some benzimidazole isosteres and this could be attributed to the steric hindrance effect of the large planer aromatic ring. Similarly, replacing the olefinic

hydrogen in oxopiperazine **9** with *p*-aminophenyl acetic acid in **10** diminished the urease-inhibitory activity to its half value. Again, the remarkable decrease of the activity between oxopiperazine analogs **9** and **10** could be attributed to the steric hindrance effect. Noticeably, oxopiperazine moiety was preferred than anthranilic acid moiety in a small nonsterically hindered molecule for the structural requirements of urease inhibition. This proposal could be supported by the poor urease inhibitory activity of the large organometallic complexes **14a**,**b** carrying bis-anthranilic acid moiety.

2.4 | Molecular modeling study

In an effort to understand the obtained biological data on a structural basis, considering the potent urease inhibitory activity of the target compounds **3** and **9–11** compared to thiourea, molecular modeling simulation was performed for all of them using molecular operating environment. Further, a comparative modeling was carried out for the inactive compound **12.** Urease cocrystallized with acetohydroxamic acid (Protein Data Bank ID: 4h9m) has been taken as a reference to control the performance of the docking approach.

Obviously, compounds **3** and **9–11**, which were superior to the standard urease inhibitor thiourea in enzyme assay, revealed much better docking scores (−8.12 to −3.07 kcal/mol), interacted strongly with both nickel atoms, Ni 901 and Ni 902, at distances less than 3 Å (2.0–2.8 Å) and were also hydrogen-bonded to amino acid residues located in the binding pocket of the enzyme. However, thiourea revealed a docking score of −0.86 kcal/mol, through only one coordination bond with nickel atom Ni 902 (2.6 Å) (Table 3).

Focusing on the binding pose of the most potent oxopiperazine **9**, the carbonyl oxygen of the ester moiety illustrated two strong coordination bonds with Ni 901 (2.5 Å) and Ni 902 (2.6 Å). In addition, the carbonyl oxygen of the oxopiperazine ring accepted one hydrogen from the NH_2 group of Arg 609 (2.5 Å). Also, the two NHs of oxopiperazine ring were hydrogen-bonded to Asp 494 and His 593 at distances 2.7 and 2.8 Å, respectively (Figure 6).

In turn, the aromatic carboxylate of compound **3** displayed two coordination bonds with the two nickel atoms, Ni 901 (2.6 Å) and Ni 902 (2.0 Å). Also, a strong hydrogen bond (2.5 Å) was observed between carboxylate OH moiety and carbonyl oxygen of Gly 550, in addition to arene-cation interaction between the phenyl moiety of compound **3** and the guanidine group of Arg 609 (Figure 6).

Noticeably, the anthranilic acid analog **3** and the phenyl acetic acid analogs **10** and **11** exhibited similar binding modes. The carboxylate group of anthranilic acid moiety in **3** and that of phenyl acetic acid moieties in **10** and **11** were coordinated to the two nickel atoms. Additionally, the two NHs of oxopiperazine ring in compound **10** formed two hydrogen bonds with Asp 494 and Cys 592 (CME 592). Similarly, compound **11** formed three hydrogen bonds with Cys 592, and His 594 by virtue of the NH and the carboxylate of anthranilic acid moiety, respectively. This similarity in binding mode may account for the equipotency of compounds **3**, **10**, and **11** as urease inhibitors (Figures 6, 7).

Focusing on benzimidazole **12**, despite having docking score much better than thiourea, it revealed no interaction with nickel atoms. The bulky benzimidazole ring was anchored to the entrance of the binding pocket, showing arene-arene interaction with the imidazole ring of His 593, and subsequently withdrawing the carboxylate group of the anthranilic acid moiety away from nickel atoms by more than 8 Å. Instead, the carboxylate group formed two hydrogen bonds with Asp 494 and His 593 (Figure 7). This could explain the inactivity of benzimidazole **12** against urease enzyme.

TABLE 3 The docking scores of compounds **3**, **9–12**, with interacting residues in the active site of jack bean urease compared to thiourea and acetohydroxamic acid.

Compound no.	Docking score (kcal/mol)	Interacting residues (distance in Å)
3	−5.73	Gly 550 (2.5)
		Arg 609 (arene-cation)
		Ni 901 (2.6)
		Ni 902 (2.0)
9	−3.07	Asp 494 (2.7)
		His 593 (2.8)
		Arg 609 (2.5)
		Ni 901 (2.5)
		Ni 902 (2.6)
10	−8.12	Asp 494 (3.1)
		Cys 592 (2.8)
		Ni 901 (2.2)
		Ni 902 (2.1, 2.3)
11	−7.69	Arg 439 (arene-cation)
		Cys 592 (2.8, 2.9)
		His 594 (2.7)
		Ni 901 (2.0, 2.8)
		Ni 902 (2.0)
12	−6.7	Asp 494 (2.9)
		His 593 (2.9)
		His 593 (arene-arene)
Thiourea[a]	−0.86	Ni 902 (2.6)
Acetohydroxamic acid[b]	−6.05	His 409 (2.6)
		Leu 490 (2.4)
		His 492 (2.9)
		Asp 633 (2.2, 2.6)
		Ni 901 (1.3)
		Ni 902 (2.7)

[a]Thiourea reference standard for in vitro urease assay.
[b]Acetohydroxamic acid cocrystallized ligand with jack bean urease enzyme in Protein Data Bank (4h9m).

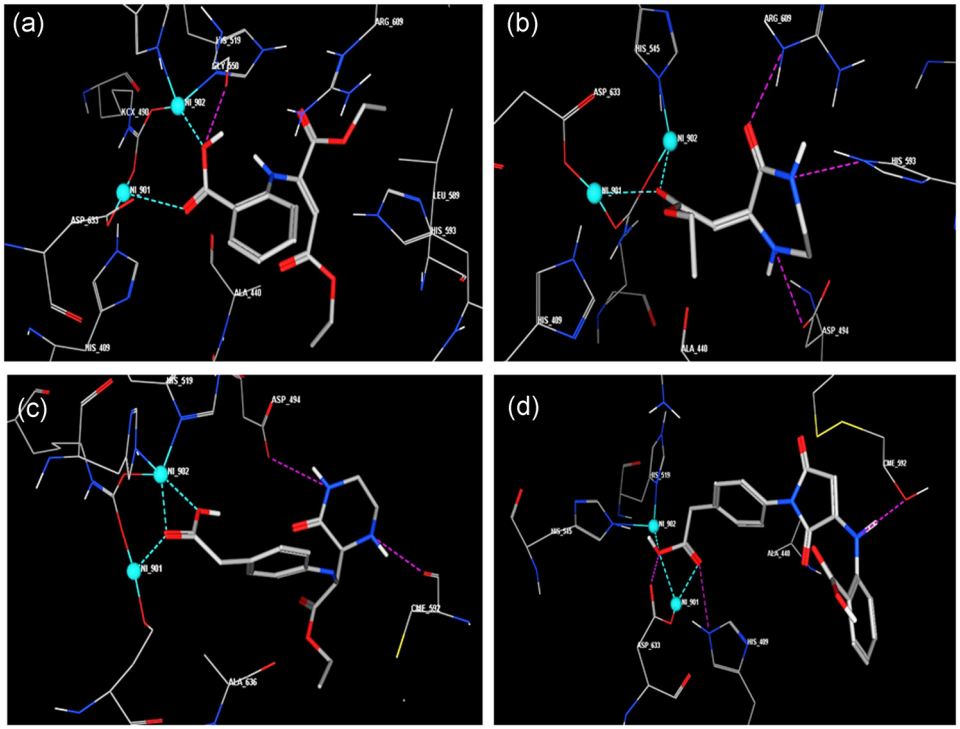

FIGURE 6 The binding mode of compounds **3** (a), **9** (b), **10** (c), and **11** (d) docked into the active site of jack bean urease enzyme (colored by atom type, light blue dashed lines for interaction with nickel atoms, purple dashed lines for hydrogen bonding, light blue balls for nickel atoms)

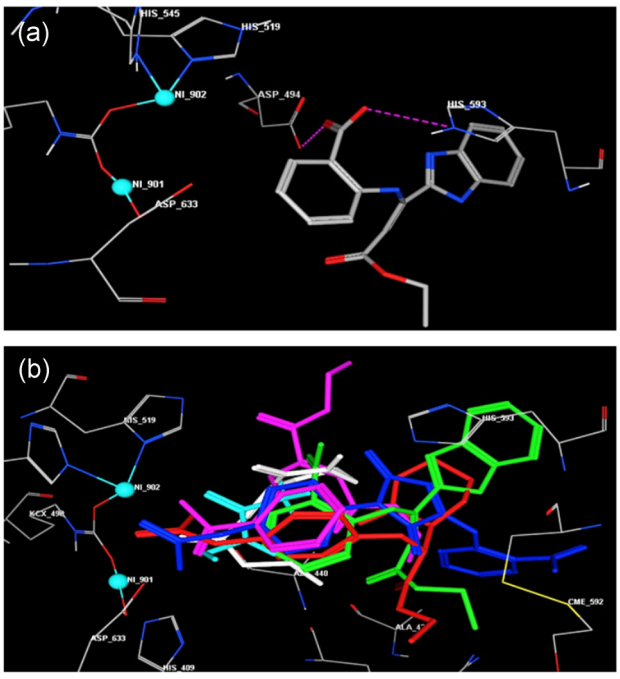

FIGURE 7 (a) The binding mode of compound **12** docked into the active site of jack bean urease enzyme. (b) Overlay of compounds **3** (purple), **9** (white), **10** (red), **11** (blue), **12** (green), and acetohydroxamic acid (light blue) docked into the active site of jack bean urease enzyme

3 | CONCLUSION

During this study, anthranilic acid and diethylacetylenedicarboxylate were used in the synthesis of new nitrogenous organo compounds under mild reaction conditions. The newly synthesized compounds were evaluated for their in vitro inhibitory potential against urease enzyme. Most compounds were identified as potent urease inhibitors. Docking studies of active compounds into the binding pocket of urease enzyme revealed a common strong interaction with nickel atoms. The docking scores, as well as the binding modes, were in agreement with the in vitro urease assay.

4 | EXPERIMENTAL

4.1 | Chemistry

4.1.1 | General

All melting points were measured on a Gallenkamp electrothermal melting point apparatus. The infrared spectra were recorded for potassium bromide pellets on a PyeUnicam SP 3-300 and FT IR 8101 PC Shimadzu infrared spectrophotometers. The ^{1}H NMR spectra were recorded in dimethylsulfoxide-d6 (DMSO-d6) at 400 MHz on Agilent Technologies Mercury NMR spectrometers. Mass spectra were recorded at 70 eV on a GCMSeQP 1000 EX Shimadzu mass spectrometer (for gas chromatography (GC)/MS) and on Agilent GC 6890 N coupled with an Agilent Mass Selective Detector 5973 (for ESI-MS). Elemental analyses were carried out at the Microanalytical

Center of Cairo University. Analyses indicated by the symbols of the elements or functions were within ± 0.4% of the theoretical values. X-ray crystallography was carried out on a Kappa CCD FR 590 diffractometer (Enraf Nonius), National Research Center, Dokki, Cairo, Egypt. DEAD and anthranilic acid were obtained from Aldrich and used without further purification. The tested compounds have a range between 95% and 100% purity.

The original spectra of the investigated compounds and detailed structural data of compounds **3**, **9**, and **14b** are provided as Supporting Information. The InChI codes of the investigated compounds together with some biological activity data are also provided as Supporting Information.

2-((1,4-Diethoxy-1,4-dioxobut-2-en-2-yl)amino)benzoic acid (3)

Compound **3** was prepared by stirring anthranilic acid **1** (1 mmol) with DEAD **2** (1 mmol) in ethanol (5 ml) at rom temperature for 2 hr. The solid formed was collected by filtration, washed with diethyl ether, dried and finally recrystallized from acetic acid to afford **3**: as yellow plates (CH_3COOH), yield (95%), mp. 158–160°C. IR (KBr) ν (cm^{-1}): 3275 (NH), 1728, 1670 (ester C=O), 1680 (acid C=O); ^{1}H NMR (DMSO-d6) δ 1.041 (t, 3H, CH_3CH_2, J = 7.2 Hz), 1.10 (t, 3H, $\underline{CH_3}CH_2$, J = 5.2 Hz), 4.08–4.17 (m, 4H, 2($CH_3\underline{CH_2}$)), 5.43 (s, 1H, vinylic CH), 6.65 (d, 1H, ArH, J = 8.4 Hz), 7.04–7.07 (m, 1H, ArH), 7.42–7.46 (m, 1H, ArH), 7.87 (d. 1H, ArH, J = 8 Hz), 8.1, 11.03 (2s, 2H, D_2O exchangeable NH, COOH). MS *m/z* (%): 308 (M^{+1}, 1.09), 307 (M^+, 5.53), 261 (2.23), 234 (80.67), 188 (52.95), 170 (14.73), and 146 (100); Anal. calcd. for $C_{15}H_{17}NO_6$ (307.10) C, 58.63; H, 5.58; N, 4.56. Found: C, 58.11; H, 5.08; N, 5.03.

4.1.2 | X-ray structure determination of compound 3

A single crystal of compound **3** was obtained by slow evaporation from acetic acid. Compound **3**: $C_{15}H_{17}NO_6$, Mr = 307.302, yellow plates, triclinic space group P$^-$1 with Z = 2, a = 8.8202(4), b = 9.6161(4), c = 10.0404(6) Å, alpha = 78.0398(14)°, beta = 69.722(2)°, gamma = 75.802(2)°, V = 767.38(7) Å^3; Dx = 1.330 Mg/m^3, μ = 0.10 mm^{-1}. The intensity data were recorded using a Bruker Noniu CCD FR 590 area-detector diffractometer,[44] with graphite monochromated Mo Kα radiation (λ = 0.71073 Å) at T = 298 K. 1657 observed reflections, θ_{max} = 27.49°; 3650 independent reflections I > 3 sigma(I), Rint = 0.024. Structure solution by direct methods full-matrix least squares refinement based on F2 and 199 parameters. All but H-atoms were refined anisotropicly. Hydrogen atoms were clearly located from difference Fourier maps, refined at idealized positions riding on the carbon atoms with isotropic displacement. Refinement converged at R(all) = 0.109, wR(all) = 0.110, S(all) = 0.782; min./max. deltaF −0.35/0.49 e/Å^3. Crystallographic data for the structural analysis of compound **3** has been deposited with the Cambridge Crystallographic Data Center (CCDC) under the number 1498175. Copies of the information may be obtained free of charge from The Director, CCDC, 12 Union Road, Cambridge CB2 1EZ, UK (http://www.ccdc.cam.ac.uk).

5-Oxo-2,5-dihydro-1*H*-pyrazole-3-carbohydrazide (6)

Compound (**6**) was prepared by mixing compound **3** (1 mmol) with excess $NH_2NH_2.H_2O$ in ethanol (10 ml) under reflux for 3 hr. The reaction mixture was cooled. The solid formed was collected by filtration, washed with ethanol and diethylether, dried and finally recrystallized from ethanol to afford **6**: as faint yellow powder (C_2H_5OH), yield 40%, mp. 243–245°C; IR (KBr) ν (cm^{-1}): 3371, 3275 (NH), 1716, 1681 (C=O); ^{1}H NMR (DMSO-d6) δ 4.45 (brs, 2H, D_2O exchangeable NH_2), 5.96 (s, 1H, vinylic CH), 9.49, 9.79, and 12.29 (3s, 3H, D_2O exchangeable NH); ^{13}C NMR (DMSO-d6) δ 86.70 (C4-pyrazoline ring), 114.47 (C3-pyrazoline ring), 161.41, 161.83 (C5-pyrazoline ring and C3-carbohydrazide); MS *m/z* (%): 143 (M^{+1}, 1.87), 142 (M^+, 19.54), 111 (85.21), 105 (3.29), 83 (18.46), 68 (16.95), 57 (11.59), 55 (81.54), 53 (100), 44 (20.56), 43.13 (32.12). Anal. calcd. for $C_4H_6N_4O_2$ (142.05) C, 33.81; H, 4.26; N, 39.42. Found: C, 34.10; H, 4.66; N, 39.10.

4.1.3 | Synthesis of ethyl 2-(3-oxopiperazin-2-ylidene)acetate (9): Method A

Compound **9** was prepared by mixing compound **3** (1 mmol) with ethylenediamine (1 mmol) in ethanol (5 ml) under reflux for 2 hr. The reaction mixture was cooled. The solid formed was collected by filtration, washed with ethanol and diethylether, dried, and finally recrystallized from ethanol to afford **9**: as yellow cubes, yield 55%, mp. 167–169°C. IR (KBr) ν (cm^{-1}): 3325, 3224 (NH), 1689, 1658 (C=O). ^{1}H NMR (DMSO-d6) δ 1.15 (t, 3H, $\underline{CH_3}CH_2$, J = 7.2 Hz), 3.25–3.29 (m, 4H, CH_2–CH_2 piprazine), 4.04 (q, 2H, CH_3–$\underline{CH_2}$, J = 7.2 Hz), 5.16 (s, 1H, vinylic CH), 8.33, 8.40 (2s, 2H, D_2O exchangeable NH). MS *m/z* (%): 184 (M^+, 10.42), 177 (33.50), 158 (11.73), 140 (31.16), 139 (100), 124 (29.87), 111 (40.54), 102 (42.21), 84 (72.44), and 75 (41.50). Anal. calcd. for $C_8H_{12}N_2O_3$ (184.08) C, 52.17; H, 6.57; N, 15.21. Found: C, 51.99; H, 6.10; N, 15.55.

4.1.4 | X-ray structure determination of compound 9

A single crystal of compound **9** was obtained by slow evaporation from ethanol. Compound **9**: $C_8H_{12}N_2O_3$, Mr = 184.195, yellow cube, monoclinic space group P2$_1$/a with Z = 4, a = 12.0301(8), b = 4.5470(3), c = 17.0770(13) Å, alpha = 90.00°, beta = 94.619(3)°, gamma = 90.00°, V = 931.09(11) Å^3; Z = 4; Dc = 1.314 Mg/m^3, μ = 0.10 mm^{-1}. The intensity data were recorded using a Bruker Nonius CCD FR 590 area-detector diffractometer[44] with graphite monochromated Mo Kα radiation (λ = 0.71073 Å) at T = 298 K. 533 reflections collected θ_{max} = 30.0°; 3257 independent reflections I > 3 sigma(I), Rint = 0.081. Structure solution by direct methods, full-matrix least squares refinement based on F2 and 118 parameters. All but H-atoms

were refined anisotropiclly. Hydrogen atoms were clearly located from difference Fourier maps, refined at idealized positions riding on the carbon atoms with isotropic displacement parameters. Refinement converged at R(all) = 0.246, wR(all) = 0.111, S(all) = 0.632; min./max. deltaF −0.60/0.56 e/Å^3. Crystallographic data for the structural analysis of compound **9** has been deposited with the CCDC under the number 1498175. Copies of the information may be obtained free of charge from The Director, CCDC, 12 Union Road, Cambridge CB2 1EZ, UK (http://www.ccdc.cam.ac.uk).

4.1.5 | Synthesis of ethyl 2-(3-oxopiperazin-2-ylidene)acetate (9): Method B

The second method for preparation of compound **9** adopted the reported literature.[31] Compound **9** was prepared by warming DEAD **2** (1 mmol) with ethylenediamine (1 mmol) in ethanol (5 ml) with stirring for 2 hr. The solid formed was collected by filtration, washed with ethanol and diethylether, dried and finally recrystallized from ethanol to afford compound **9**: as faint yellow flakes, yield 65%, mp. 167–169°C.

2-(4-((2-Ethoxy-2-oxo-1-(3-oxopiperazin-2-yl)ethyl)amino)phenyl)acetic acid (10)

Compound **10** was prepared by mixing compound **9** (1 mmol) with *p*-aminophenyl acetic acid (2 mmol) in ethanol (5 ml) under reflux for 6 hr (TLC-control). The reaction mixture was cooled. The solid formed was collected by filtration, recrystallized from ethanol to afford **10** as brown powder; yield 80%, mp. > 350°C. IR (KBr) ν (cm^{-1}): 3367, 3336, 3305 (OH, NH), 1705, 1689 and 1658 (C=O). ^{1}H NMR (DMSO-d6) δ 1.03 (t, 3H, $\underline{CH_3}CH_2$, J = 8 Hz), 1.13 (brs, 1H, D_2O exchangeable OH), 3.25–3.42 (m, 10H; 4H, CH_2-CH_2piprazine, 1H, CH ethyl, 1H, CH piperazinyl, 2H, $\underline{CH_2}$COOH and 2H, $CH_3\underline{CH_2}$), 6.46 (d, 2H, ArH, J = 8.4 Hz), 6.85 (d, 2H, ArH, J = 8.4 Hz), 6.99, 7.00 (2s, 2H, D_2O exchangeable NH), 8.50 (brs, 1H, D_2O exchangeable $\underline{COOH}$). ^{13}C NMR (DMSO-d6) δ 19 ($COOCH_2\underline{CH_3}$), 40.59, 40.63 (C2,5,6 piperazine, $\underline{CH_2}$-COOH), 56.46 ($COO\underline{CH_2}CH_3$, C1 ethyl), 114, 126, 129, 130 (Ar C), 148 (C–OH, piperazine C3), 160 (CO, $CH_2\underline{COOH}$ and $\underline{COO}C_2H_5$), MS *m/z* (%): 336 (M^{+1}, 25.67), 320 (M^+–CH_3, 1.72), 313 (100), 305 (6.01), 290 (2.25), 285 (26.84), 264 (17.18), 262 (11.79), 184 (3.01), 150 (11.17), 109 (15.14). Anal. calcd. for $C_{16}H_{21}N_3O_5$ (335.15) C, 57.30; H, 6.31; N, 12.53. Found: C, 57.00; H, 6.10; N, 12.63.

2-((1-(4-(Carboxymethyl)phenyl)-2,5-dioxo-2,5-dihydro-1*H*-pyrrol-3-yl)amino) benzoic acid (11)

Compound **11** was prepared by mixing compound **3** (1 mmol) with *p*-aminophenyl acetic acid (1 mmol) in ethanol (5 ml) under reflux for 4 hr (TLC-control). The reaction mixture was cooled. The solid formed was collected by filtration, recrystallized from ethanol to afford **11**: as yellow powder, yield 83%, mp. 184–186°C. IR (KBr) ν (cm^{-1}): 3394, 3367 (NH), 1705, 1651 (C=O). ^{1}H NMR (DMSO-d6) δ 3.37 (s, 2H; $\underline{CH_2}$–COOH), 3.5 (brs, 1H, D_2O exchangeable $\underline{COOH}$), 5.78 (s, 1H, vinylic CH), 6.50 (d, 2H, ArH, J = 8.4 Hz), 6.87 (d, 2H, ArH, J = 8 Hz), 7.18–7.40 (m, 4H, ArH), 9.8 (s, 1H, D_2O exchangeable NH). ^{13}C NMR (DMSO-d6) δ 40.59 ($\underline{CH_2}$–COOH), 114.28, 120.08, 120.54, 122.31, 126.95, 130.07, 130.14, 130.27, 130.42, 130.73, 131.11, 138.33, 147.55 (Ar C and vinylic C), 167.01, 172.00 (CO imide), 173.14, 173.82 (CO, $\underline{COOH}$), MS *m/z* (%): 366 (M^+, 6.34), 365 (45.77), 335 (100), 319 (41.73), 313 (15), 311 (11.33), 111 (19.00), 302 (18.10), 301 (10.73), 273 (10.72), 254 (16.51), 231 (11.26), 150 (17.75), 122 (10.88). Anal. calcd. for $C_{19}H_{14}N_2O_6$ (366.09) C, 62.30; H, 3.85; N, 7.65. Found: C, 62.50; H, 3.96; N, 7.42.

2-((1-(1*H*-Benzo[*d*]imidazol-2-yl)-3-ethoxyprop-1-en-1-yl)amino)benzoic acid (12)

Compound **12** was prepared by mixing compound **3** (1 mmol) with *o*-phenylenediamine (1 mmol) in ethanol (5 ml) under reflux for 3 hr (TLC-control). The reaction mixture was cooled. The solid formed was collected by filtration, recrystallized from ethanol to afford **12** as yellow crystals: yield 88%, mp. 210–212°C. IR (KBr) ν (cm^{-1}): 3367, 3265 (NH), 1685, 1651 (C=O). ^{1}H NMR (DMSO-d6) δ 1.18 (t, 3H, $\underline{CH_3}CH_2$, J = 7.2 Hz), 4.10 (q, 2H, $CH_3\underline{CH_2}$, J = 7.2 Hz), 5.47 (s, 1H, vinylic CH), 6.99–7.06 (m, 4H, ArH), 7.25–7.31 (m, 2H, ArH), 7.51 (t, 1H, ArH, J = 1.6 Hz), 7.71 (d, 1H, ArH, J = 8.8 Hz). MS *m/z* (%): 352 (M^{+1}, 1.66), 351 (M^+, 1.81), 322 (1.75), 308 (2.20), 306 (1.87), 237 (1.60), 204 (2.20), 186 (7.92), 160 (10.75), 131 (19.03), 80 (64.59), 64 (100). Anal. calcd. for $C_{19}H_{17}N_3O_4$ (351.12) C, 64.95; H, 4.88; N, 11.96. Found: C, 64.82; H, 4.38; N, 12.46.

Tri-aqua *bis*(2-acetylaminobenzoato)Zn(II), [Zn($C_9H_8NO_3$)$_2$(H_2O)$_3$](H_2O)$_2$ (14a)

The complex **14a** was prepared by dissolving $Zn(NO_3)_2.4H_2O$ (1 mmol) in distilled water (10 ml). Then, solution of 1 M NaOH was added portionwise until the formation of the gelatinous hydrated zinc hydroxide was completed. The resulting mixture was centrifuged and the solid was washed thoroughly with distilled water (6 × 5 ml). The wet gelatinous solid was suspended in distilled water (25 ml). Then it was added to a solution of acetyl anthranilic acid (1 mmol) in ethanol (10 ml) with stirring. A glossy white precipitate of zinc complex appeared after a few seconds, filtered and washed several times with water and ethanol to afford **14a** as fine white crystal: yield 50%, mp. > 300°C. Anal. calcd. for $C_{18}H_{26}N_2O_{11}Zn$; (510.08) C, 42.24; H, 5.12; N, 5.47. Found: C, 42.74; H, 5.32; N, 5.07.

Tri-aqua *bis*(2-acetylaminobenzoato)Cu(II), [Cu($C_9H_8NO_3$)$_2$(H_2O)$_3$](H_2O)$_2$ (14b)

The complex **14b** was prepared by dissolving $CuSO_4.5H_2O$ (1.5 mmol) in distilled water (10 ml). The salt solution was added to a solution of acetyl anthranilic acid (1 mmol) in ethanol (10 ml) with stirring. The metal complex was precipitated after addition of small aliquots of 1 M NaOH to afford **14b** as green crystals: yield 30%, mp. > 300°C. Anal. calcd. for $C_{18}H_{26}N_2O_{11}Cu$; (509.08) C, 42.39; H, 5.14; N, 5.49. Found: C, 42.21; H, 4.82; N, 6.05.

4.1.6 | X-ray structure determination of copper complex 14b

Here the single crystal of **14b** proved a mononuclear geometrical structure. The copper atom existed in a central symmetrical position in pentadentate coordination system. There are two coordination bonds shared by two oxygen atoms of the carboxylate ions. So, each carboxylate group bound in a mono dentate manner and the other three coordination bonds shared by three water molecules. In this case the geometry was best described as tetrahedral. The arrangement was completed by existence of another two water molecules at the top of the crystal geometry.

A single crystal of compound **14b** was obtained by slow evaporation from a mixture of ethanol/water (1:1). Compound **14b**: $C_{18}H_{26}N_2O_{11}Cu$, Mr = 419.874, green prismatic crystal, orthorhombic space group $P2_12_12_1$ with Z = 4; a = 7.1674(2), b = 17.3033(6), c = 18.3535(9) Å, alpha = 90.00°, beta = 90.00°, gamma = 90.00°. V = 2276.2(2) $Å^3$; D_x = 1.225 Mg/m^3, μ = 0.99 mm^{-1}, The intensity data were recorded using a Bruker Nonius CCD FR 590 area-detector diffractometer[44] with graphite monochromated Mo Kα radiation (λ = 0.71073 Å) at *T* = 298 K. 1726 observed reflections, θ = 2.910–27.485°; 3185 independent reflections I > 3 sigma (I), Rint = 0.042. Structure solution by direct methods, full-matrix least squares refinement based on F2 and 289 parameters. All but H-atoms were refined anisotropiclly. Hydrogen atoms were clearly located from difference Fourier maps, refined at idealized positions riding on the carbon atoms with isotropic displacement parameters. Refinement converged at R(all) = 0.097, wR(all) = 0.107, S(all) = 2.025; min./max. deltaF −0.78/0.72 e/$Å^3$. Crystallographic data for the structural analysis of compound **14b** has been deposited with the CCDC under the number 766987. Copies of the information may be obtained free of charge from The Director, CCDC, 12 Union Road, Cambridge CB2 1EZ, UK (http://www.ccdc.cam.ac.uk).

4.2 | Urease inhibition assay

The urease activity was determined by measuring the amount of ammonia being produced using indophenol method described by Weatherburn.[45,46] Briefly, the assay mixture, containing 10 µL of urease *Canavalia ensiformis* (jack bean urease, Sigma) and 10 µL of test compound in 40 µL phosphate buffer containing 100 mM urea were incubated for 30 min at 37°C in 96-well plates. 40 µL each of phenol reagents (1%, w/v phenol and 0.005%, w/v sodium nitroprusside) and 40 µL of alkali reagent (0.5%, w/v NaOH and 0.1% active chloride NaOCl) were added to each well. The absorbance at 625 nm was measured after 30 min, using a microplate reader (BioTekELx 800, Instruments, Inc.). All reactions were performed in triplicate. Thiourea was used as the standard inhibitor of urease. The IC_{50} values were determined by the nonlinear curve fitting program PRISM 5.0 (GraphPad, San Diego, CA).

ACKNOWLEDGMENT

The authors express deep thanks to Dr. Abdel-Sattar S. Hamad Elgazwy for his valuable instructions to get the single crystal of compound **14b** with CCDC under the number 766987.

CONFLICT OF INTERESTS

The authors have declared that there is no conflict of interest.

ORCID

Heba S.A. El-Zahabi http://orcid.org/0000-0002-7023-6364
Hanan G. Abdulwahab http://orcid.org/0000-0003-3035-2624

REFERENCES

[1] H. L. Mobley, R. P. Hausinger, *Microbiol. Rev.* **1989**, *53*, 85.
[2] C. R. Carlini, R. Ligabue-Braun, *Toxicon* **2016**, *110*, 90. https://doi.org/10.1016/j.toxicon.2015.11.020
[3] R. A. Burne, Y. Y. M. Chen, *Microbes Infect.* **2000**, *2*, 533. https://doi.org/10.1016/S1286-4579(00)00312-9
[4] C. Follmer, *J. Clin. Pathol.* **2010**, *63*, 424. https://doi.org/10.1136/jcp.2009.072595
[5] P. Kosikowska, Ł. Berlicki, *Expert Opin. Ther. Pat.* **2011**, *21*, 945. https://doi.org/10.1517/13543776.2011.574615
[6] A. M. Felix, L. B. Czyzewski, D. P. Winter, R. I. Fryer, *J. Med. Chem.* **1969**, *12*, 384.
[7] A. Eudes, E. E. K. Baidoo, F. Yang et al., *Appl. Microbiol. Biotechnol.* **2011**, *89*, 989. https://doi.org/10.1007/s00253-010-2939-y
[8] S. Tayyab, M. S. Zaroog, S. R. Feroz, S. B. Mohamad, S. N. A. Malek, *Int. J. Pharm.* **2015**, *491*, 352. https://doi.org/10.1016/j.ijpharm.2015.06.042
[9] M. Isaji, H. Miyata, Y. Ajisawa, Y. Takehana, N. Yoshimura, *Br. J. Pharmacol.* **1997**, *122*, 1061. https://doi.org/10.1517/13543776.2011.574615
[10] A. Rauf, S. Shahzad, M. Bajda et al., *Bioorg. Med. Chem.* **2015**, *23*, 6049.
[11] T. Tanaka, M. Kawase, S. Tani, *Life Sci.* **2003**, *73*, 2985.
[12] P. Kafarski, M. Talma, *J. Adv. Res.* **2018**, *13*, 101. https://doi.org/10.1016/j.jare.2018.01.007
[13] A. Ibrar, I. Khan, N. Abbas, *Arch. Pharm. (Weinheim)* **2013**, *346*, 423. https://doi.org/10.1002/ardp.201300041
[14] K. Macegoniuk, R. Kowalczyk, A. Rudzińska, M. Psurski, J. Wietrzyk, Ł. Berlicki, *Bioorg. Med. Chem. Lett.* **2017**, *27*, 1346.
[15] M. Tsuchiya, L. Imamura, J. Park, K. Kobashi, *Biol. Pharm. Bull.* **1995**, *18*, 1053.
[16] J. B. Park, L. Imamura, K. Kobashi, *Biol. Pharm. Bull.* **1996**, *19*, 182.
[17] S. T. S. Hassan, M. Žemlička, *Arch. Pharm. (Weinheim)* **2016**, *349*, 507.
[18] M. Taha, A. Wadood, *Bioorg. Chem.* **2018**, *78*, 411.
[19] D. M. S. Vardhan, H. K. Kumara, H. P. Kumar, D. C. Gowda, *Int. J. Pharm. Pharm. Sci.* **2017**, *9*, 92.
[20] Z. -L. You, L. -L. Ni, D. -H. Shi, S. Bai, *Eur. J. Med. Chem.* **2010**, *45*, 3196.
[21] Y. M. Cui, X. W. Dong, W. Chen, W. J. Wang, Y. G. Li, H. L. Zhu, *J. Enzyme Inhib. Med. Chem.* **2012**, *27*, 528.
[22] D. Ali, S. Kazem, R. I. Mohammad, *ARKIVOC* **2007**, *i*, 180.
[23] F. I. Zubkov, V. P. Zaitsev, A. A. Orlova, A. S. Peregudov, N. M. Mikhailova, A. V. Varlamov, *Russ. J. Org. Chem.* **2007**, *43*, 1202.
[24] A. Komaraiah, K. Ramakrishna, B. Sailu, P. S. N. Reddy, *ARKIVOC* **2007**, *xiv*, 110.

[25] O. S. Eltsov, M. V. Smirnova, Y. Yu. Morzherin, N. P. Belskaiya, V. S. Mokrushin, *ARKIVOC* **2008**, *xvii*, 306.
[26] J. Crosby, M. C. McKie, R. M. Paton, J. F. Ross, *ARKIVOC* **2000**, *v*, 720.
[27] J. F. Ross, C. Delipala, M. C. Watson, J. Crosby, R. M. Paton, *ARKIVOC* **2013**, *iii*, 372.
[28] S. K. Khetan, M. V. George, *Can. J. Chem.* **1969**, *47*, 3545.
[29] N. D. Heindel, P. D. Kennewell, M. Pfau, *J. Chem. Soc. D* **1969**, 757.
[30] J. Wu, S. Kang, Q. Yuan et al., *Molecules* **2012**, *17*, 9413.
[31] Y. Iwanami, Y. Kenjo, K. Nishibe, M. Kajiura, S. Isoyama, *Bull. Chem. Soc. Jpn.* **1964**, *37*, 1740.
[32] S. M. Medvedeva, K. S. Shikhaliev, *J. Mater. Sci. Eng.* **2015**, *5*, 310.
[33] Y. A. Ammar, M. M. F. Ismail, M. K. Ibrahim, H. S. A. El-Zahaby, *Afinidad* **2005**, *62*, 151.
[34] O. V. Shekhter, N. L. Sergovskaya, Yu. S. Tsizin, *Chem. Heterocycl. Compd.* **1985**, *21*, 665.
[35] I. Vlahou, N. Kourkoumelis, A. Michaelides, S. Skoulika, J. C. Plakatouras, *Inorg. Chim. Acta* **2006**, *359*, 3540.
[36] L. Naso, A. C. González Baró, L. Lezama, T. Rojo, P. A. M. Williams, E. G. Ferrer, *J. Inorg. Biochem.* **2009**, *103*, 219.
[37] J. B. Sumner, *J. Biol. Chem.* **1926**, *69*, 435.
[38] S. Ciurli, S. Benini, W. R. Rypniewski, K. S. Wilson, S. Miletti, S. Mangani, *Coord. Chem. Rev.* **1999**, *190–192*, 331.
[39] C. Follmer, F. V. Pereira, N. P. da Silveira, C. R. Carlini, *Biophys. Chem.* **2004**, *111*, 79.
[40] L. Sheridan, C. M. Wilmot, K. D. Cromie, S. Van der Logt, S. Phillips, *Acta Crystallogr. Sect. D* **2002**, *58*, 374.
[41] C. Follmer, *Phytochemistry* **2008**, *69*, 18.
[42] S. Shabana, A. Kawai, K. Kai, K. Akiyama, H. Hayashi, *Biosci. Biotechnol. Biochem.* **2010**, *74*, 878.
[43] K. M. Khan, F. Rahim, A. Khan et al., *Bioorg. Med. Chem.* **2014**, *22*, 4119.
[44] S. Mackay, C. J. Gilmore, C. Edwards, N. Stewart, K. Shankland, *maXus Computer Program for the Solution and Refinement of Crystal Structures*, MacScience, Japan and The University of Glasgow, Bruker Nonius, The Netherlands **1999**.
[45] M. W. Weatherburn, *Anal. Chem.* **1967**, *39*, 971.
[46] M. A. S. Aslam, S. U. Mahmood, M. Shahid, A. Saeed, J. Iqbal, *Eur. J. Med. Chem.* **2011**, *46*, 5473.

SUPPORTING INFORMATION

Additional supporting information may be found online in the Supporting Information section at the end of the article.

How to cite this article: El-Zahabi HSA, Abdulwahab HG, Edrees MM, Hegab AM. Utility of anthranilic acid and diethylacetylenedicarboxylate for the synthesis of nitrogenous organo/organometallic compounds as urease inhibitors. *Arch. Pharm. Chem. Life Sci.* 2019;e1800314. https://doi.org/10.1002/ardp.201800314